International Journal of Bifurcation and Chaos, Vol. 24, No. 11 (2014) 1450147 (12 pages)

DOI: 10.1142/S0218127414501478

Bifurcation Results for Traveling Waves in Nonlinear Magnetic Metamaterials

M. Agaoglou and V. M. Rothos
Department of Mathematics, Physics Computational Sciences, Faculty of Engineering, Aristotle University of Thessaloniki, Thessaloniki 54124, Greece

D. J. Frantzeskakis and G. P. Veldes
Department of Physics, University of Athens, Panepistimiopolis, Zografos, Athens 15784, Greece

H. Susanto
Department of Mathematical Sciences, University of Essex, Wivenhoe Park, Colchester CO4 3SQ, UK

Received May 5, 2014

In this work, we study a model of a one-dimensional magnetic metamaterial formed by a discrete array of nonlinear resonators. We focus on periodic and localized traveling waves of the model, in the presence of loss and an external drive. Employing a Melnikov analysis we study the existence and persistence of such traveling waves, and study their linear stability. We show that, under certain conditions, the presence of dissipation and/or driving may stabilize or destabilize the solutions. Our analytical results are found to be in good agreement with direct numerical computations.

Keywords: Resonator; metamaterials; periodic waves; localized waves; Melnikov function.

1. Introduction

Magnetic metamaterials (MMs) are metamaterials consisting of periodic arrays of split-ring resonators (SRRs), in one-, two- and three dimensions [Marques *et al.*, 2008]. Both the dimensions of SRRs and their inter-space distance are small relative to the free space wavelength and, thus, the quasi-magnetostatic approximation [Jackson, 1999] governs the dynamics of electromagnetic (EM) fields in such settings. As shown in earlier works [Shamonina *et al.*, 2002a, 2002b], MMs support magneto-inductive (MI) waves, due to the coupling between SRRs (which can be modeled as LC circuits). In fact, MI waves are found in the short wavelength limit, which means that MI waves are slow waves: their phase velocity and the group velocity are smaller than the velocity of light in free space. Magnetic metamaterials have attracted much interest as they have already been used for the realization of various microwave devices, including couplers and splitters [Shamonina & Solymar, 2004], shifters [Nefedov & Tretyakov, 2005], delay lines [Freire *et al.*, 2004], parametric amplifiers [Sydoruk *et al.*, 2007], magneto-inductive lenses [Freire & Marques, 2008], polarizers [Gansel *et al.*, 2009], and so on.

Nonlinear MMs, which can be implemented by embedding the array of SRRs into a nonlinear dielectric [Zharov *et al.*, 2003; Shadrivov *et al.*, 2006a] or by inserting diodes into resonant conductive elements [Lapine *et al.*, 2003; Shadrivov *et al.*, 2006b], have also been studied in various works. The latter method can more easily be implemented

in practice — see, e.g. relevant experimental works on three-dimensional ("metacrystal") MMs [Huang *et al.*, 2010] and on the modulation instability in MM waveguides [Tamayama *et al.*, 2013]. In such settings, various studies have been performed, including the localization of EM energy and the formation of discrete breathers [Lazarides *et al.*, 2006], magneto-inductive envelope solitons [Kourakis *et al.*, 2007] and gap solitons [Cui *et al.*, 2007], transfer of EM power in MM transmission lines [Lazarides *et al.*, 2011] and others.

In this paper, we consider periodic and localized traveling waves in a one-dimensional (1D) nonlinear MM, composed by a chain of nonlinear SRRs. In particular, we study the persistence of the waves in the presence of perturbations, namely dissipations and traveling drives. This is done by employing a Melnikov-type of analysis, which is complemented by computing the existence and stability of the solutions numerically. The present study extends our previous work [Diblik *et al.*, 2014] on the analysis of a 1D MM with Kerr-type materials by considering a quadratic nonlinearity of the system. More specifically, our presentation is organized as follows. In Sec. 2, we present the physical model. In Sec. 3, we study periodic traveling waves under the assumption that the unperturbed system has periodic solutions. We find conditions under which these periodic solutions persist using the subharmonic Melnikov bifurcation method. In Sec. 4, we consider the persistence of a localized wave that is the limiting case of the periodic solutions. In Sec. 5, we present numerical computations comparing the analytical results in the preceding sections. Additionally, we also consider the existence and stability of solutions due to the periodic traveling drive, whose amplitude is limited by the magnitude of the forcing. Finally, Sec. 6 summarizes our findings.

2. The Nonlinear Magnetic Metamaterial Model

We consider a nonlinear MM, composed by an infinite 1D chain of identical nonlinear circular SRRs, as shown in Fig. 1(top). Each of the SRRs is modeled by a resonant circuit, namely a LC circuit, and the nonlinearity in the model is assumed to be introduced by inserting a diode in the slit of SRR — cf. Fig. 1(bottom); this way, the total effective capacitance of SRR becomes nonlinear (see details below). Furthermore, each SRR in the chain is driven

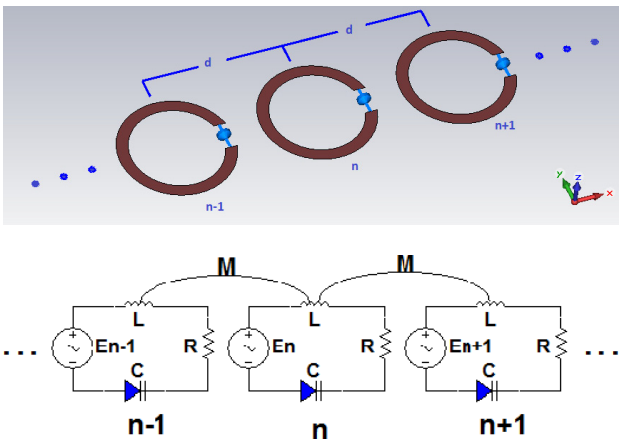

Fig. 1. (Top) A representative illustration of the nonlinear magnetic metamaterial structure. (Bottom) The equivalent circuit model (see text for details).

by the electromotive force $E_n(t)$, which is induced by an external EM field. The SRRs are assumed to be magnetically coupled, i.e. via the mutual inductance M between two inductors; here, solely such next-nearest-neighbor interactions will be considered. Finally, we note that dissipative effects will also be taken into account, accounted for by the finite conductivity of the metallic SRR structure.

Let us now consider the electric analogue of the model. According to, e.g. [Lapine *et al.*, 2003], each SRR can be modeled by an effective RLC circuit, characterized by the ohmic resistance R, the self-inductance L, and a capacitance C, which is a combination of the linear capacitance $C_{\rm sl}$ due to the slit of the SRR and the effective capacitance of the inserted diode [Carbonell *et al.*, 2008]. The latter is biased at a constant voltage, say U_0, and its capacitance is nonlinear, depending on the voltage U applied across it. Assuming that this voltage U does not change significantly from the bias voltage U_0, we can Taylor expand the effective capacitance $C(U_n)$ of the nth SRR taking into regard only the lowest order terms, namely,

$$C(U_n) \approx C_0 + C_0' U_n = C_0(1 + \alpha U_n), \qquad (1)$$

where $C_0 \equiv C(U_0) + C_{\rm sl}$, $C_0' \equiv (dC/dU)|_{U_0}$, and $\alpha = C_0'/C_0$. Taking into regard the above expression, the application of Kirchhoff's voltage law for the nth SRR [see Fig. 1(bottom)] leads to the following equation for the voltage:

$$U_n + L\frac{dI_n}{dt} + RI_n - M\frac{dI_{n-1}}{dt} - M\frac{dI_{n+1}}{dt} - E_n(t) = 0, \qquad (2)$$

where

$$I_n = \frac{dQ_n}{dt} = \frac{d}{dt}[C(U_n)U_n], \tag{3}$$

is the current of the nth SRR, and we have taken into regard that the mutual inductance M is negative in the coplanar configuration of Fig. 1.

For our considerations below, we will now derive an equation for the charge Q_n of the capacitor of the nth SRR, similarly to what was done in [Lazarides *et al.*, 2011]. Taking into regard that the charge Q_n is given by:

$$Q_n = C(U_n)U_n = C_0(1 + \alpha U_n)U_n, \tag{4}$$

we solve Eq. (4) with respect to U_n up to the order $\mathcal{O}(Q_n^2)$, and substituting the resulting expression into Eq. (2), we obtain the following equation for Q_n:

$$L\frac{d^2}{dt^2}(Q_n - \lambda Q_{n-1} - \lambda Q_{n+1}) + R\frac{dQ_n}{dt} + U_n - E_n(t) = 0, \tag{5}$$

where $\lambda = M/L$ is the coupling coefficient. Next, we introduce the scale transformations $u_n = U_n(U_c)^{-1}$, $q_n = Q_n(C_0U_c)^{-1}$ (where U_c is the breakdown potential of the diode), and $t \to \omega_0 t$ [where $\omega_0^2 = (LC_0)^{-1}$], and cast Eq. (5) into the following form:

$$\frac{d^2}{dt^2}(q_n - \lambda q_{n-1} - \lambda q_{n+1}) + \gamma\frac{dq_n}{dt} + q_n - \beta q_n^2 - \varepsilon_n(t) = 0, \tag{6}$$

where $\beta = \alpha U_c$, $\gamma = RC_0\omega_0$ is the loss coefficient and $\varepsilon_n = U_c^{-1}E_n$ is the normalized electromotive force.

3. Bifurcation Results for Traveling Waves

In this section, we focus on a traveling drive h, which is C^2-smooth and 2π-periodic, i.e.

$$\varepsilon_n(t) = h(z), \quad z = \omega t + pn, \tag{7}$$

where $\omega > 0$ is the external driving frequency, $p \neq 0$ is the wavenumber of the driving wave field, $n \in \mathbb{Z}$ and $t \in \mathbb{R}$ is the evolution time. Assuming that $q_n(t) = U(z)$, with $U \in C^2(\mathbb{R}, \mathbb{R})$, we obtain from (6) the following advance-delay equation:

$$\begin{aligned}\omega^2 U''(z) + U(z) - \beta U^2(z) \\ - \epsilon\lambda\omega^2[U''(z-p) + U''(z+p)] \\ + \epsilon\gamma\omega U'(z) - \epsilon h(z) = 0,\end{aligned} \tag{8}$$

where we have considered that parameters γ, λ and the drive are small, $\propto \epsilon$ (where ϵ is a nonzero formal small parameter).

3.1. *Case 1*: *Periodic traveling waves*

We now make the following assumptions:

(H1) $U''(z) - \varphi(U(z)) = 0$ (where φ is the nonlinearity of the magnetic material, which is normally assumed to be of Kerr-type [Lazarides *et al.*, 2006] and in our case $\varphi = -U(z) + \beta U^2(z)$ has a $\overline{T}$-periodic solution U_0.

Remark 3.1. Since $U_0(-z + c_0)$ also solves $U''(z) + U(z) - \beta U^2(z) = 0$ and there is $z_0 \in \mathbb{R}$ such that $U_0'(z_0) = 0$, we may suppose that $U_0(0) = 0$ and then $U_0(z) = U_0(-z)$. Then

$$U_\omega(z) := U_0\Big(\frac{z}{\omega}\Big)$$

satisfies $\omega^2 U_\omega''(z) + U_\omega(z) - \beta U_\omega^2(z) = 0$. Note U_ω is $T_\omega := \overline{T}\omega$-periodic and even.

We also assume the resonance condition

(H2) $T_\omega = 2\pi u/v$ for $u, v \in \mathbb{N}$, and because of that we will study the case with $v = 1$.

The assumption (H2) then becomes

(H3) $\omega = 2\pi u/\overline{T}$ for $u \in \mathbb{N}$.

We now apply the standard subharmonic Melnikov method to (8) based on the Lyapunov–Schmidt method [Diblik *et al.*, 2014]; we compute that the Melnikov function is given by:

$$M^u(a) = -\gamma\int_0^{\overline{T}} U_0'(z)^2 dz - \frac{2\pi u}{\overline{T}}\int_0^{\overline{T}} h'\Big(\frac{2\pi u}{\overline{T}}z + a\Big)U_0(z)dz. \tag{9}$$

From (H1), we obtain

$$\frac{1}{2}(U')^2 + \Big(\frac{U^2}{2} - \frac{\beta U^3}{3}\Big) = c_0,$$

where c_0 is a constant. The above equation has a one-parameter family of periodic solutions [Byrd & Friedman, 1954]

$$U_{0,\alpha}(z) = A\frac{1-\mathrm{cn}\left(\frac{z}{g}\right)}{1+\mathrm{cn}\left(\frac{z}{g}\right)} + \alpha,$$

where cn is the cnoidal Jacobi elliptic function, and g, α are constants (see details in Appendix A).

For $\alpha > 0$ with periods $\overline{T} = \overline{T(\alpha)} = 4K(k)g$ (where $K(k)$ is the complete elliptic function of the first kind, and k the elliptic modulus), we can compute the first term on the right-hand side of the Melnikov function (9) as

$$\int_0^{\overline{T}(\alpha)} U'_{0,\alpha}(z)^2 dz = \frac{4A^2}{g^2}\int_0^{\overline{T}(\alpha)} \frac{\mathrm{sn}^2\left(\frac{z}{g}\right)\mathrm{dn}^2\left(\frac{z}{g}\right)}{\left(1+\mathrm{cn}\left(\frac{z}{g}\right)\right)^4} dz = \frac{4A^2}{g}\int_0^{4K(k)} \frac{\mathrm{sn}^2(z)\mathrm{dn}^2(z)}{(1+\mathrm{cn}(z))^4} dz$$

$$= \frac{4A^2}{g}\frac{((-1+2k)E(\mathrm{am}(4K(k),k),k) - 4(-1+k)K(k))}{3(1+\mathrm{cn}(z))^4 k},$$

where sn and dn are Jacobi elliptic functions and am is the Jacobi amplitude.

Similarly, by taking

$$h(z) = \cos z, \tag{10}$$

we can evaluate the remaining term of the function (9) as explained in Appendix B; the result is:

$$\frac{2\pi u}{\overline{T}(\alpha)}\int_0^{\overline{T}(\alpha)} h'\left(\frac{2\pi u}{\overline{T}(\alpha)}z + a\right) U_{0,\alpha}(z) dz = \frac{A\pi u}{2K(k)}\Xi \sin a, \tag{11}$$

where

$$\Xi = \frac{P}{24\pi^5 u^5 K^5(k)} \tag{12}$$

and

$$P = -(64\pi u\cos(2\pi u K^2(k))K(k)^2(24 - 48k + \pi^2 u^2 K^2(k)(-3 + 16(-1+2k)K(k)^2)) + 32(-24 + 48k$$
$$+ \pi^2 u^2 K^2(k)(3 + K^2(k)(48 - 96k + 2\pi^2 u^2 K^2(k)(-3 + 8(-1+2k)K^2(k)))))\sin(2\pi u K(k)^2)). \tag{13}$$

Here, we have used the fact that $\cos(z), \mathrm{cn}(z)$ are even and $\sin(z)$ is odd and made the expansion of $-1 + \frac{2}{(1+\mathrm{cn}(z))}$.

Summing up the contributions above, the Melnikov function is then given by

$$M^u(a) = -\gamma\int_0^{\overline{T}} U'_0(z)^2 dz - \frac{2\pi u}{\overline{T}}\int_0^{\overline{T}} h'\left(\frac{2\pi u}{\overline{T}}z + a\right) U_0(z) dz$$

$$= -\gamma\frac{4A^2}{g}\left[\frac{((-1+2k)E(\mathrm{am}(4K(k),k),k) - 4(-1+k)K(k))}{3(1+\mathrm{cn}(z))^4 k}\right] + \frac{A\pi u}{2K(k)}\Xi\sin a. \tag{14}$$

Theorem 1. *Suppose (H1) and (H2). If there is a simple zero a_0 of a Melnikov function, i.e. $M^{u/v} = 0$ and $D_a M^{u/v}(a_0) \neq 0$, then there is a $\delta > 0$ such that for any $0 \neq \varepsilon \in (-\delta, \delta)$ there is a unique $2\pi u$-periodic*

solution $U(z)$ of (8) with

$$U(z) = U_0\left(\frac{z-a_0}{\omega}\right) + O(\varepsilon).$$

To have a simple zero of $M^u(a)$, we need

$$\gamma\Lambda(\alpha, u) < 1,$$

where

$$\Lambda(\alpha,u) := \frac{\dfrac{4A^2}{g}\left[\dfrac{((-1+2k)E(\mathrm{am}(4K(k),k),k) - 4(-1+k)K(k))}{3(1+\mathrm{cn})^4 k}\right]}{\dfrac{A\pi u}{2K(k)}\Xi}.$$

Thus, we see that

$$\gamma < \frac{1}{\Lambda(\alpha,u)} \tag{15}$$

gives the magnitude for the damping in order to apply Theorem 1.

3.2. *Case 2: Localized traveling waves*

For localized traveling waves, instead of (H1) we have the following assumption:

(C1) $\varphi(0) = 0$, $\varphi'(0) < 0$ and $U''(z) - \varphi(U(z)) = 0$ (where in our case $\varphi = -U(z) + \beta U^2(z)$) has an asymptotic localized solution $\Gamma \in C^2(\mathbb{R},\mathbb{R})$ such that $\lim_{|z|\to+\infty}\Gamma(z) = 0$ and $\lim_{|z|\to+\infty}\Gamma'(z) = 0$.

Now, we apply the standard homoclinic Melnikov method to Eq. (8), based on the Lyapunov–Schmidt method [Diblik *et al.*, 2014], and we get the Melnikov function:

$$M(a) = \int_{-\infty}^{\infty}(-\gamma\Gamma'(z) + h(\omega z + a))\Gamma'(z)dz. \tag{16}$$

The unperturbed equation possesses a homoclicic solution:

$$\Gamma(z) = \frac{1}{\beta} - \frac{3\,\mathrm{sech}^2\left(\dfrac{z}{2}\right)}{2\beta}.$$

Using again Eq. (10) for the form of the drive, the Melinkov function (16) becomes:

$$\begin{aligned} M(a) &= \int_{-\infty}^{\infty}(-\gamma\Gamma'(z) + h(\omega z + a))\Gamma'(z)dz \\ &= -\frac{6(\gamma + 5\beta\pi\omega^2\,\mathrm{csch}(\pi\omega)\sin(a))}{5\beta^2}. \end{aligned} \tag{17}$$

Theorem 2. *Suppose (C1). If there is a simple zero a_0 of the Melnikov function*

$$M(a) = \int_{-\infty}^{\infty}(-\gamma\Gamma'(z) + h(\omega z + a))\Gamma'(z)dz$$

then there is $\theta > 0$ such that for any $0 \neq \varepsilon \in (-\theta,\theta)$ there is a unique bounded solution $U(z)$ of (8) on $\mathbb{R}$ with

$$U(z) = \Gamma\left(\frac{z-a_0}{\omega}\right) + O(\varepsilon).$$

Therefore, if we want the Melnikov function $M(a)$ to have a simple zero we need

$$\gamma < 5\beta\pi\omega^2\,\mathrm{csch}(\pi\omega). \tag{18}$$

Note that $M(a)$ gives a kind of $O(\epsilon)$-measure of the distance between the stable and unstable manifolds of the periodic solution U_0 of our perturbed system which is at a $O(\epsilon)$-distance from U_0. Thus, if $M(a)$ has a simple zero at some points, as in our case, the implicit function theorem implies that these two manifolds intersect transversally along a solution φ which is homoclinic to U_0.

4. Numerical Results

To illustrate the theoretical results obtained in the previous section, we have solved the model equation in a moving coordinate frame [cf. Eq. (8)] numerically. The advance-delay equation under consideration is solved using a pseudo-spectral method, i.e. we express the solution U in a Fourier series

$$U(z) = \sum_{j=1}^{J}[A_j\cos((j-1)\tilde{k}z) + B_j\sin(j\tilde{k}z)], \tag{19}$$

where $\tilde{k} = 2\pi/L$ and $-L/2 < z < L/2$. The Fourier coefficients A_j and B_j are then found by requiring the series to satisfy (8) at several collocation points. Hence, $2J$ collocation points are required, which are chosen with uniform grid points. Typically, we use $J = 50$. It is important to note that the physically relevant range for the coupling parameter λ is $|\lambda| < 1/2$ [Diblik *et al.*, 2014].

The stability of a solution obtained from (8) is then determined numerically through calculating its Floquet multipliers χ, which are eigenvalues of the monodromy matrix. As a first-order system, the linearized equation of (6) is:

$$\begin{aligned} \dot{u}_n &= v_n, \\ \dot{v}_n - \lambda\dot{v}_{n-1} - \lambda\dot{v}_{n+1} &= -\gamma v_n - u_n + 2\beta U_n u_n, \end{aligned} \tag{20}$$

where $U_n(t) = U(\omega t + np)$ [cf. (19)] is a periodic solution of (6). The linear system is integrated using a Runge–Kutta method of order four with periodic boundary conditions over the period $\overline{T} = L/\omega$. The monodromy matrix $\mathcal{M}$ is defined as

$$\begin{pmatrix} \{u_n(T)\} \\ \{v_n(T)\} \end{pmatrix} = \mathcal{M} \begin{pmatrix} \{u_n(0)\} \\ \{v_n(0)\} \end{pmatrix}.$$

A periodic solution is unstable if there is any Floquet multiplier that is strictly greater than one in modulus. The typical dynamics of the instability is demonstrated by integrating the governing equation (6) using the same numerical method.

Without loss of generality, below we fix $\beta = 1$. Considering a simple periodic drive in (10), we take

$$h(z) = \Delta\cos(z), \tag{21}$$

where $\Delta \in \mathbb{R}$ is the driving amplitude.

4.1. *Persistence and stability of traveling waves of the unperturbed system*

In this part, we will study the persistence of periodic or localized traveling waves of the unperturbed system in the presence of small perturbations described in the preceding sections and the stability of the perturbed solutions. To do so, it is firstly important to understand the effect of each perturbation term in the governing equation (6).

In Fig. 2(a) we show the solution profile of the advance-delay equation (8) with $\Delta = \gamma = \lambda = 0$ and $\overline{T} = 4\pi$. Turning on the perturbation by setting only one of the parameters (Δ, γ, or λ) nonzero, one would expect that the solution will persist. This is indeed the case, except for the case of $\gamma \neq 0$, $\Delta = 0$; physically speaking, this can be understood by the fact that damping will dissipate energy and drive is needed to compensate the dissipation. Mathematically this is in agreement with Eq. (15), which will be discussed further.

When the perturbation is small enough, the profile of the solution will be very similar to the unperturbed case. However, the stability can change drastically. Shown in Fig. 2(b) are the Floquet multipliers of the perturbed solution when the oscillators are decoupled, i.e. $\lambda = 0$. Using several values of Δ (and $\gamma = 0$), we conclude that the drive pulls the multipliers along the unit circle and later destabilize the solution through a period-doubling bifurcation. As for the effect of coupling on the stability of solutions, we plot in Fig. 2(c) the Floquet multipliers of the solution corresponding to that in panel (a) for two values of λ and $\gamma = 0$. As seen, the coupling creates a band of multipliers and for the present parameter values destabilizes solutions. Combining the two effects, the dynamics of the multipliers are nontrivial and one may obtain either a stable or unstable periodic solution, as depicted also in panel (c). When we obtain stable solutions, the stabilization is clearly due to the drive. This result is similar to the stabilization of unstable discrete solitary waves in parametrically driven oscillators reported in [Syafwan *et al.*, 2010; Susanto *et al.*, 2006].

As for the dissipation, it may yield asymptotic stability. However, to stabilize unstable solutions by increasing the dissipation parameter, the solutions may already cease to exist before all corresponding unstable Floquet multipliers enter the unit circle. This is due to the bound that is predicted by (15); see also (18) for localized waves. In the following, we will compare the prediction with our numerics.

Shown in Fig. 3(a) is the bifurcation diagram of the solution corresponding to Fig. 2(a) as a function of the dissipation parameter γ for a fixed value of Δ and λ. As γ increases from zero, there is a saddle-node bifurcation. Following the existence branches further, we obtain the full diagram as presented in the figure, where there is a pair of saddle-node bifurcations and the diagram is symmetric with respect to the vertical line $\gamma = 0$. Comparing with the analytical approximation (15) (for the sake of simplicity

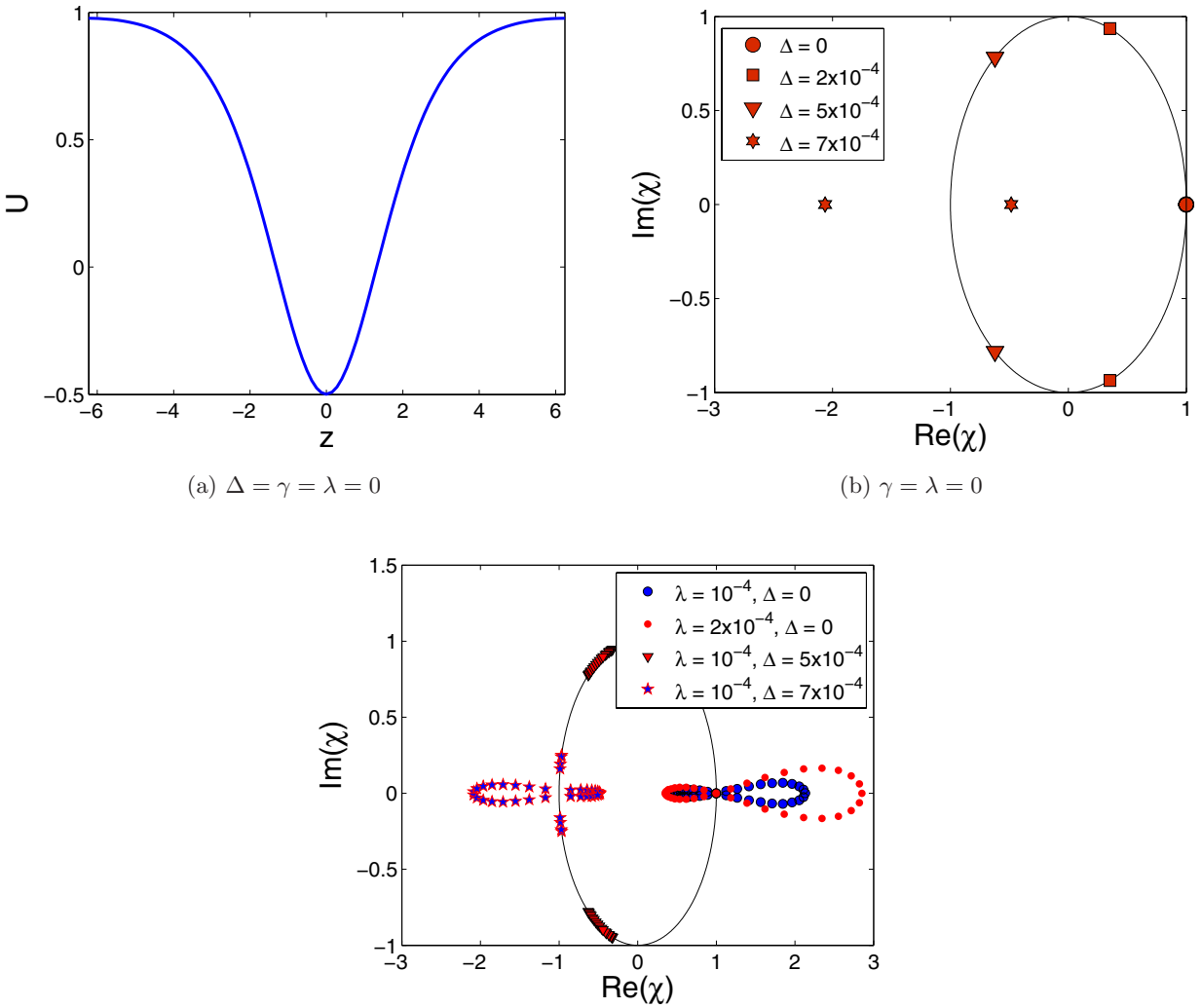

(a) $\Delta = \gamma = \lambda = 0$

(b) $\gamma = \lambda = 0$

(c) $\gamma = 0$

Fig. 2. (a) A periodic wave in a traveling frame. (b)–(c) Floquet multipliers of the solution corresponding to panel (a) for parameter values as given in the captions. The solution period in all the plots is $\overline{T} = 4\pi$. As a guide we also plot the unit circle in thin solid curve. The stability is calculated using 20 sites.

we use (18) instead) shown as vertical dashed line in the figure, we obtain a satisfactory agreement. As for the solution profile along the bifurcation diagram, by visual observation only, we obtain that the solution is shifted to the left in z as γ changes and due to the periodicity returns to its initial position after completing one full bifurcation loop.

In addition to the existence, we also investigated the stability. Despite the symmetry of the existence diagram, the stability is expectedly asymmetric. The stability of the corresponding solution is indicated by the solid curve in Fig. 3(a). In this case, we obtain that the damping can indeed stabilize solutions. However, this is not necessarily always the case. When, e.g. the coupling parameter λ is large enough, we obtain that all corresponding solutions along the bifurcation diagram can be unstable. In Fig. 3(b), we show a typical dynamics of unstable solutions.

The existence and stability dynamics of solutions due to the perturbation above are rather general and independent of the period $\overline{T}$. Nevertheless, we observe that the larger the period, the more unstable the solution. In the same effect as the case of large enough λ that we mentioned above, the presence of dissipation may not be able to stabilize the corresponding solutions in their entire existence domain. Therefore, using the same argument, we expect that the localized wave is always unstable. This is due to the fact that the solution background,

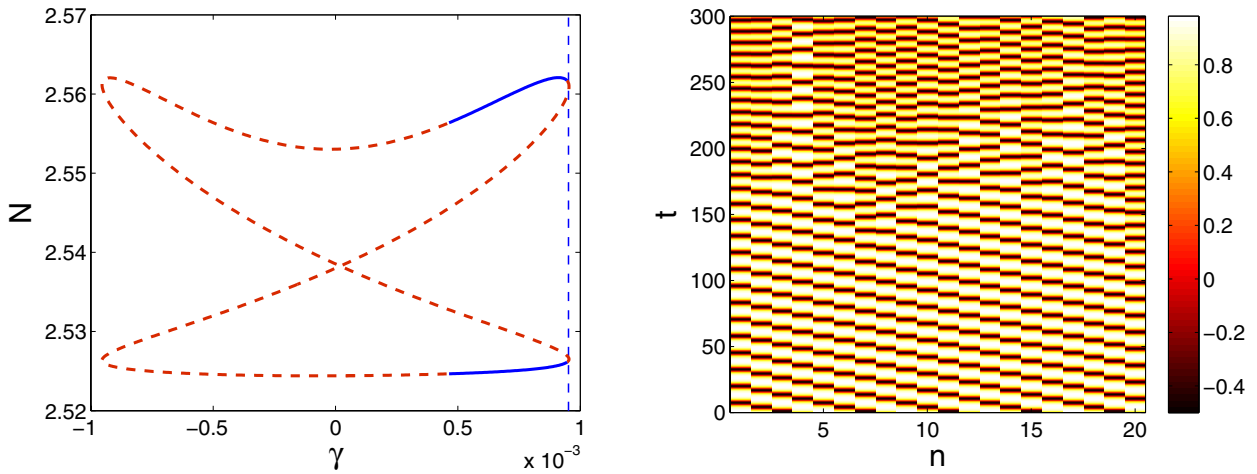

(a) (b)

Fig. 3. (a) Bifurcation diagram of the solution corresponding to Fig. 2(a) with $\Delta = 7 \times 10^{-4}$ and $\lambda = 10^{-4}$. The vertical axis is the solution norm $N = \sqrt{\int_0^{\overline{T}} U(z)^2 dz}$. Solid and dashed curves indicate stable and unstable solutions, respectively. The stability is calculated using 20 sites. The vertical dashed line is the prediction (18). (b) Typical dynamics of the instability. The initial condition is the solution obtained immediately after the first bifurcation point in (a).

when unperturbed, is a saddle-point. Moreover, the instability in this case is typically in the form of an unbounded blow-up, similarly to that found in [Diblik *et al.*, 2014].

4.2. *Periodic waves due to drives*

In addition to the periodic and localized waves discussed in the previous subsection, one also has periodic solutions due to the traveling drive. In this case, the amplitude of the solutions is proportional to the drive amplitude. Such solutions were not discussed analytically here. However, the regularity and uniqueness result of [Diblik *et al.*, 2014] for this type of solutions is immediately applicable to our case. Therefore, for the sake of completeness, we also discuss them here.

In Fig. 4, we show one example of the existence and stability of periodic waves due to the traveling drive. In panel (a), one can observe that for

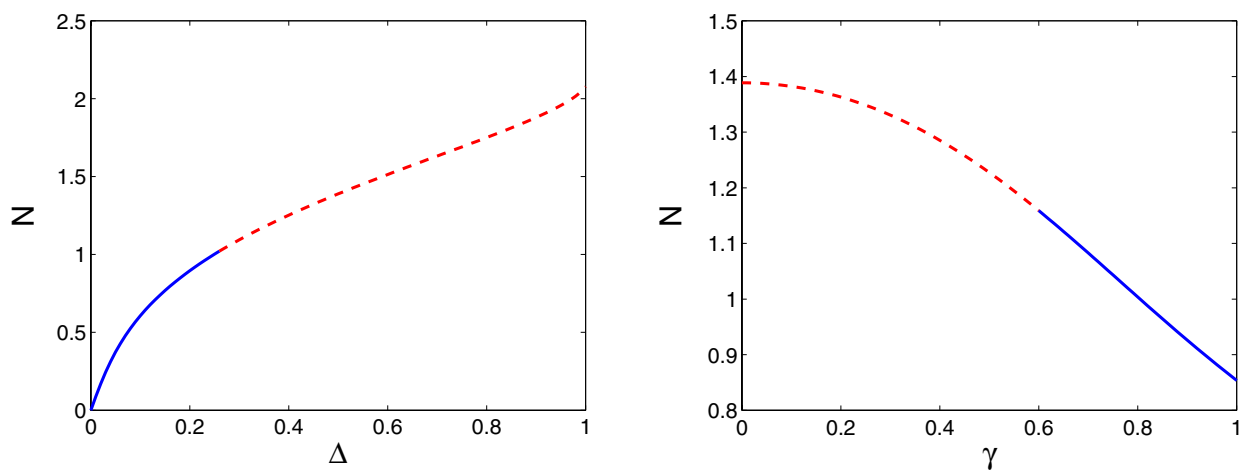

(a) (b)

Fig. 4. (a)–(b) The existence curve of periodic waves due to the traveling drive for (a) varying Δ with $\gamma = 0$ and $\lambda = 0.1$; (b) varying γ with $\Delta = 0.5$ and $\lambda = 0.1$. The vertical axis is the solution norm $N = \sqrt{\int_0^{\overline{T}} U^2(z) dz}$. Solid and dashed curves indicate stable and unstable solutions, respectively. The stability is calculated using 20 sites. (c) The solution profile with $\Delta = 0.5$, $\lambda = 0.1$, and $\gamma = 0.57$. (d) The Floquet multipliers of the solution in panel (c), showing the instability of the solution.

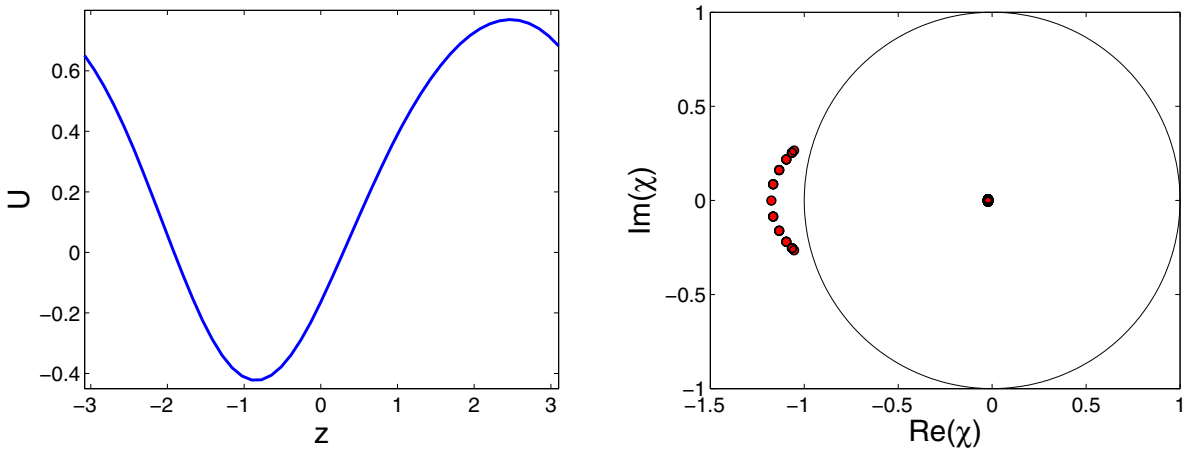

(c) (d)

Fig. 4. (*Continued*)

small enough driving amplitude the solution is stable. When it is increased further, there is a critical drive amplitude above which the solution becomes unstable. The reason is the same as that in Fig. 2, i.e. the drive creates an instability caused by multipliers leaving the unit circle from -1. Introducing the dissipation γ, one can stabilize unstable solutions. Shown in panel (b) is the existence and stability diagram for varying γ, where the stabilization effect can readily be observed. In panel (c), we plot the profile of an unstable solution for one set of parameter values. The multiplier structure in the complex plane is depicted in panel (d).

The time evolution of the unstable solution in Fig. 4(c) is shown in Fig. 5. The dynamics, where one or more sites blow up, is typical for this type of waves.

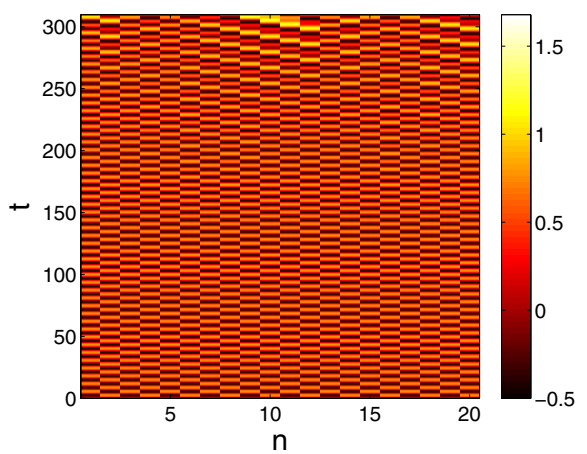

Fig. 5. Typical dynamics of the instability of a periodic wave due to the drive. The initial condition corresponds to the solution plotted in Fig. 4(c).

5. Conclusion

Using a Melnikov-type analysis we have discussed analytically the existence of periodic and localized traveling waves in an array of magnetic metamaterials. Intrinsic characteristics of the system, such as the coupling coefficient and the loss coefficient, affect the stability of the system. Our analysis showed that even if we have instability, under certain conditions, we can make our solution stable by adjusting the amplitude of driving. We have also used direct numerical simulations to compare and confirm the above analytical result. Moreover, by computing the Floquet multipliers of the periodic solutions we also determined the stability of the solutions. It was shown that the traveling drive can act both as a stabilizer and as a destabilizer. In addition, periodic waves with amplitude being proportional to the drive strength were also studied numerically. In this case, we observed that due to the loss, an unstable solution can be stabilized.

It would be particularly interesting to follow the lines of the present study and analyze similar models which appear in the context of nonlinear metamaterials. Indeed, such nonlinear lattice models appear in the context of nonlinear left-handed transmission line metamaterials [Marques *et al.*, 2008] and have been studied also in experiments (see, e.g. [Kozyrev & van der Weide, 2008; Ogaswara & Narahara, 2010; English *et al.*, 2011]). In most of the relevant settings, the focus was on the reduction of the lattice model to an effective nonlinear Schrödinger (NLS) equation, by means of which approximate soliton solutions of the original model

were presented. Nevertheless, our analysis may be extremely useful in identifying traveling periodic wave or other (than envelope solitons) localized solutions, and studying their persistence and stability. Work is in progress towards this direction and relevant results will be reported elsewhere.

Acknowledgments

The work of M. Agaoglou has been co-financed from resources of the operational program "Education and Lifelong Learning" of the European Social Fund and the National Strategic Reference Framework (NSRF) 2007–2013 within the framework of the Action State Scholarships Foundation's (IKY) mobility grants program for the short term training in recognized scientific/research centers abroad for candidate doctoral or postdoctoral researchers in Greek universities or research centers. The work of V. M. Rothos has been co-financed by the European Union (European Social Fund ESF) and Greek national funds through the Operational Program Education and Lifelong Learning of the National Strategic Reference Framework (NSRF) Research Funding Program: THALES Investing in knowledge society through the European Social Fund. The work of D. J. Frantzeskakis was partially supported by the Special Account for Research Grants of the University of Athens.

References

Byrd, P. F. & Friedman, M. D. [1954] *Handbook of Elliptic Integrals for Engineers and Physicists*, Die Grundlehren der Mathematischen Wissenschaften, Vol. 67 (Springer, Berlin, Heidelberg).

Carbonell, J., Boria, V. E. & Lippens, D. [2008] "Nonlinear effects in split ring resonators loaded with heterostructure barrier varactors," *Microwave Opt. Tech. Lett.* **50**, 474.

Cui, W., Zhu, Y., Li, H. & Liu, S. [2007] "Self-induced gap solitons in nonlinear magnetic metamaterials," *Phys. Rev. E* **80**, 036608.

Diblik, J., Feckan, M., Pospisil, M., Rothos, V. M. & Susanto, H. [2014] "Travelling waves in nonlinear magnetic metamaterials," in *Localized Excitations in Nonlinear Complex Systems*, Nonlinear Systems and Complexity, Vol. 7, eds. R. Carretero-Gonzalez *et al.* (Springer International Publishing, Switzerland).

English, L. Q., Wheeler, S. G., Shen, Y., Veldes, G. P., Whitaker, N., Kevrekidis, P. G. & Frantzeskakis, D. J. [2011] "Backward-wave propagation and discrete solitons in a left-handed electrical lattice," *Phys. Lett. A* **375**, 1242.

Freire, M. J., Marques, R., Medina, F., Laso, M. A. G. & Martin, F. [2004] "Planar magnetoinductive wave transducers: Theory and applications," *Appl. Phys. Lett.* **85**, 4439.

Freire, M. J. & Marques, R. [2008] "Optimizing the magnetoinductive lens: Improvement, limits, and possible applications," *J. Appl. Phys.* **103**, 013115.

Gansel, J. K., Thiel, M., Rill, M. S., Decker, M., Bade, K., Saile, V., Von Freymann, G., Linden, S. & Wegener, M. [2009] "Gold helix photonic metamaterial as broadband circular polarizer," *Science* **325**, 1513.

Huang, D., Poutrina, E. & Smith, D. R. [2010] "Analysis of the power dependent tuning of a varactor-loaded metamaterial at microwave frequencies," *Appl. Phys. Lett.* **96**, 104104.

Jackson, J. D. [1999] *Classical Electrodynamics*, 3rd edition (John Wiley and Sons, NJ).

Kourakis, I., Lazarides, N. & Tsironis, G. P. [2007] "Self-focusing and envelope pulse generation in nonlinear magnetic metamaterials," *Phys. Rev. E* **75**, 067601.

Kozyrev, A. B. & van der Weide, D. W. [2008] "Nonlinear left-handed transmission line metamaterials," *J. Phys. D* **41**, 173001.

Lapine, M., Gorkunov, M. & Ringhofer, K. H. [2003] "Nonlinearity of a metamaterial arising from diode insertions into resonant conductive elements," *Phys. Rev. E* **67**, 065601R.

Lazarides, N., Eleftheriou, M. & Tsironis, G. P. [2006] "Discrete breathers in nonlinear magnetic metamaterials," *Phys. Rev. Lett.* **97**, 157406.

Lazarides, N., Paltoglou, V. & Tsironis, G. P. [2011] "Nonlinear magnetoinductive transmission lines," *Int. J. Bifurcation and Chaos* **21**, 2147.

Marques, R., Martin, F. & Sorolla, M. [2008] *Metamaterials with Negative Parameters. Theory, Design, and Microwave Applications* (John Wiley and Sons, NJ).

Nefedov, I. S. & Tretyakov, S. A. [2005] "On potential applications of metamaterials for the design of broadband phase shifters," *Microwave Opt. Tech. Lett.* **45**, 98.

Ogasawara, J. & Narahara, K. [2010] "Experimental characterization of left-handed transmission lines with regularly spaced Schottky varactors," *IEICE Electron. Expr.* **7**, 608.

Shadrivov, I. V., Morrison, S. K. & Kivshar,Y. S. [2006a] "Tunable split-ring resonators for nonlinear negative-index metamaterials," *Opt. Expr.* **14**, 9344.

Shadrivov, V., Zharov, A. A., Zharova, N. A. & Kivshar, Y. S. [2006b] "Nonlinear magnetoinductive waves and domain walls in composite metamaterials," *Photon. Nanostruct. Fund. Appl.* **4**, 69.

Shamonina, E., Kalinin, V. A., Ringhofer, K. H. & Solymar, L. [2002a] "Magneto-inductive waveguide," *Electron. Lett.* **38**, 371.

Shamonina, E., Kalinin, V. A., Ringhofer, K. H. & Solymar, L. [2002b] "Magneto-inductive waves in one, two and three dimensions," *J. Appl. Phys.* **92**, 6252.

Shamonina, E. & Solymar, L. [2004] "Magneto-inductive waves supported by metamaterial elements: Components for a one-dimensional waveguide," *J. Phys. D: Appl. Phys.* **37**, 362.

Syafwan, M., Susanto, H. & Cox, S. M. [2010] "Discrete solitons in electromechanical resonators," *Phys. Rev. E* **81**, 026207-14.

Sydoruk, O., Shamonina, E. & Solymar, L. [2007] "Parametric amplification in coupled magnetoinductive waveguides," *J. Phys. D: Appl. Phys.* **40**, 6879.

Susanto, H., Hoq, Q. E. & Kevrekidis, P. G. [2006] "Stability of discrete solitons in the presence of parametric driving," *Phys. Rev. E* **74**, 067601–4.

Tamayama, Y., Nakanishi, T. & Kitano, M. [2013] "Observation of modulation instability in a nonlinear magnetoinductive waveguide," *Phys. Rev. B* **87**, 195123.

Zharov, A. A., Shadrivov, I. V. & Kivshar, Y. S. [2003] "Nonlinear properties of left-handed metamaterials," *Phys. Rev. Lett.* **91**, 037401.

Appendix A

Elliptic Functions

For the calculation of the Melnikov function we have used the following integral, involving the square root of three linear factors $\sqrt{t-\alpha}, \sqrt{t-b}$ and $\sqrt{t-c}$. One of the limits of the integration will usually be taken as a zero of the polynomial under the radical sign, while the other limit is considered variable. However, it may easily be used when neither limit is fixed.

$$\int_a^y \frac{dt}{\sqrt{(t-\alpha)[(t-b_1)^2+a_1^2]}} = g\int_0^{u_1} du = gu_1 = g\,\mathrm{cn}^{-1}(\cos\phi, k)$$

where

$$\mathrm{cn}\,u = \frac{A+\alpha-t}{A-\alpha+t}, \quad k^2 = \frac{A+b_1-\alpha}{2A}, \quad g = \frac{1}{\sqrt{A}},$$

$$A^2 = (b_1-\alpha)^2 + a_1^2,$$

$$(t-b)(t-c) = (t-b)(t-\bar{b}) = (t-b_1)^2 + a_1^2,$$

$$a_1^2 = -\frac{(b-\bar{b})^2}{4}, \quad b_1 = \frac{b+c}{2} = \frac{b+\bar{b}}{2},$$

$$\phi = \mathrm{am}\,u_1 = \cos^{-1}\left(\frac{A+\alpha-y}{A-\alpha+y}\right), \quad \mathrm{cn}\,u_1 = \cos\phi.$$

Here, α is real, b, c are complex and $y > \alpha$.

Appendix B

The Second Term of the Melnikov Function

The second term of the Melnikov function is found as follows:

$$\frac{2\pi u}{\overline{T}(\alpha)}\int_0^{\overline{T}(\alpha)} h'\left(\frac{2\pi u}{\overline{T}(\alpha)}z + a\right) U_{0,\alpha}(z)dz$$

$$= -\frac{2\pi u}{\overline{T}(\alpha)}\int_0^{\overline{T}(\alpha)} \sin\left(\frac{2\pi u}{\overline{T}(\alpha)}z + a\right)\left(\frac{A\left(1-\mathrm{cn}\left(\frac{z}{g}\right)\right)}{1+\mathrm{cn}\left(\frac{z}{g}\right)} + \alpha\right) dz$$

$$= -\frac{2A\pi u}{\overline{T}(\alpha)}\int_0^{\overline{T}(\alpha)} \sin\left(\frac{2\pi u}{\overline{T}(\alpha)}z + a\right)\left(\frac{\left(1-\mathrm{cn}\left(\frac{z}{g}\right)\right)}{1+\mathrm{cn}\left(\frac{z}{g}\right)}\right) dz - \frac{2\alpha\pi u}{\overline{T}(\alpha)}\int_0^{\overline{T}(\alpha)} \sin\left(\frac{2\pi u}{\overline{T}(\alpha)}z + a\right) dz$$

$$= -\frac{A\pi u}{2K(k)}\int_0^{4K(k)} \sin\left(\frac{2\pi u}{\overline{T}(\alpha)}z + a\right)\left(\frac{1-\mathrm{cn}(z)}{1+\mathrm{cn}(z)}\right) dz$$

$$= -\frac{A\pi u}{2K(k)}\left(\sin a \int_{-2K(k)}^{2K(k)} \cos\left(\frac{\pi u}{2K(k)}z\right)\left(\frac{1-\mathrm{cn}(z)}{1+\mathrm{cn}(z)}\right)dz\right.$$

$$\left. + \cos a \int_{-2K(k)}^{2K(k)} \sin\left(\frac{\pi u}{2K(k)}z\right)\left(\frac{1-\mathrm{cn}(z)}{1+\mathrm{cn}(z)}\right)dz\right)$$

$$= -\frac{A\pi u}{2K(k)}\sin a \int_{0}^{4K(k)} \cos\left(\frac{\pi u}{2K(k)}z\right)\left(\frac{1-\mathrm{cn}(z)}{1+\mathrm{cn}(z)}\right)dz$$

$$= -\frac{A\pi u}{2K(k)}\sin a \int_{0}^{4K(k)} \cos\left(\frac{\pi u}{2K(k)}z\right)\left(-1+\frac{2}{(1+\mathrm{cn}(z))}\right)dz$$

$$= \frac{A\pi u}{2K(k)}\sin a\Xi.$$